JOURNAL OF AIRCRAFT
Vol. 48, No. 1, January–February 2011

Experimental Testing of a Parametric-Model-Based Takeoff Performance Monitoring Strategy

Shane D. Pinder*
Defiant Engineering, Inc., Willowdale, Ontario, M2N 4J8 Canada
and
Trever G. Crowe† and Peter N. Nikiforuk‡
University of Saskatchewan, Saskatoon, Saskatchewan, S7N 5A9 Canada

DOI: 10.2514/1.C000222

The purpose of an aircraft takeoff performance monitoring system is to provide to the pilot information pertaining to the level of safety with which a takeoff is proceeding. The concept of a takeoff performance monitoring system is not new. Instruments have been developed and flight-tested. However, the inclusion of a takeoff performance monitoring system as a standard instrument has yet to be embraced by manufacturers and operators. A simple theoretical dynamic model was developed to investigate the feasibility of using an observer system during the roll and takeoff phases of aircraft operation to provide to the pilot the information that is needed to maneuver safely. The viability of this simple model was validated using a prototype device installed in a 19-passenger commercial turboprop aircraft. Unlike previous work in this field, the Global Positioning System was proposed as the sole source of kinematic information. This provided the possibility that a takeoff performance monitoring system could be devised that would require no additional ground-based installation. A Global Positioning System receiver and data acquisition system were installed in an aircraft operated by an airline servicing far-northern Canadian airports. The experimental investigation that was conducted to validate the theoretical model and signal processing technique showed that it was possible to predict the displacement of an aircraft to within 15 m, the length of the test aircraft, in sufficient time to aid the pilot in decision-making.

Nomenclature

A	=	frontal area of an object
a	=	acceleration of an aircraft in the direction of motion
c, d	=	constants defined in the text
D	=	force due to aerodynamic drag
D_1, D_2, D_3	=	constants in a function modeling aerodynamic drag
F	=	force due to aircraft landing-gear friction
F_2	=	constant in a function modeling landing-gear friction
j	=	tangential jerk, where jerk is the first time derivative of acceleration
k	=	subscript identifying the time step in a discrete filter
P_1, P_2, P_3	=	constants in a function modeling acceleration
q	=	zero-mean random variable describing process noise
s	=	one-dimensional displacement
T	=	force due to engine thrust
T_1, T_2, T_3	=	constants in a function modeling engine thrust
t	=	time elapsed since a reference event
V_1	=	critical engine-failure recognition speed
v	=	speed of an aircraft relative to the ground
v_a	=	component of wind velocity in the direction of aircraft motion
$v_{/a}$	=	speed of an aircraft relative to a moving mass of air
W	=	force due to weight
W_1	=	constant in a function modeling weight
ρ_{air}	=	density of air

Presented as Paper 2001-4374 at the AIAA Modeling and Simulation Technologies Conference and Paper 2001-4170 at the AIAA Guidance, Navigation, and Control Conference, Montreal, Canada, 6–9 August 2001; received 8 December 2009; revision received 21 September 2010; accepted for publication 22 September 2010.

*Director of Research; Senior Lecturer, Auckland University of Technology, Auckland, New Zealand.
†Professor, College of Engineering.
‡Dean Emeritus, College of Engineering.

I. Introduction

AIRCRAFT landing and takeoff performance monitoring is an area of research aimed at improving the information available to the pilot for decision-making during takeoff or landing. In secluded far-northern regions, where a monitoring system would be particularly useful given adverse weather, few airports are equipped to attempt frictional measurements. In such instances, a monitoring system would need to be totally self-contained and able to determine aircraft ground speed, acceleration, and position relative to the end of the runway. Prediction of the location of the aircraft at rest is then possible, with reference to a dynamic model of the aircraft. The authors have proposed that a Global Positioning System (GPS) receiver be used to determine aircraft acceleration, ground speed, and position relative to the end of the runway. A practical evaluation [1] of the feasibility of this proposal showed clear superiority of a GPS-derived acceleration over a more traditional method employing accelerometers. Advantages of the GPS-derived measurement included a modest noise level, insusceptibility to gravity and temperature-influenced variations, and far simplified mounting requirements.

Landing and takeoff performance monitoring systems are aimed at averting runway overrun. In northern regions, this has been identified [2] as a common problem. Typical causes of runway overrun include engine failure on takeoff and reduced braking resulting from runway contamination. The loss of MK Airlines flight 1608 in October 2004 and the investigation that resulted led the Canadian Transportation Safety Board to recommend the adoption of takeoff performance monitoring technology in transport aircraft [3]. Recent efforts relevant to the development of a takeoff performance monitoring system (TOPMS) [4–6] have now been given greater attention.

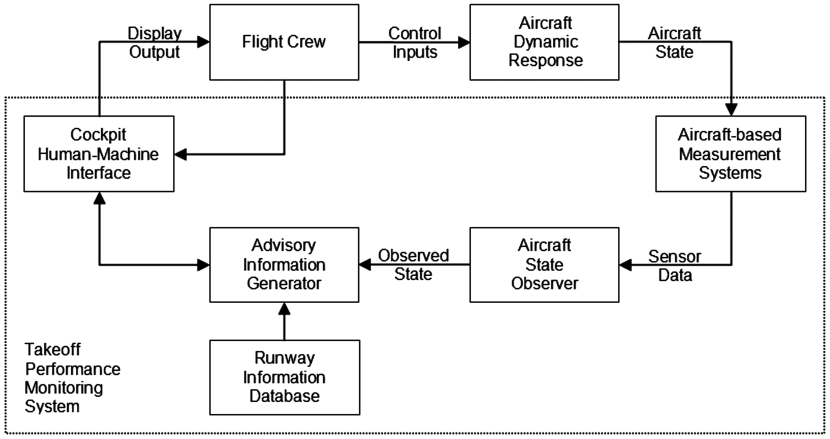

Fig. 1 TOPMS system block diagram.

A block diagram of a TOPMS is shown in Fig. 1. Control inputs supplied by the flight crew affect the dynamic state of the aircraft. Measurement systems based in the aircraft provide information regarding the aircraft state to a state observer. The observed state, together with runway information, is used to determine advisory information to be conveyed to the flight crew, using a cockpit human–machine interface. In this paper, we examine a particular approach to the measurement systems and state observer that could be used in certain circumstances.

The critical engine-failure recognition speed (V_1) is defined as the speed above which takeoff could safely continue if the most critical engine failed [7]. V_1 is often calculated before startup based on aircraft parameters and estimation of runway and weather conditions. In the event that the aircraft has reached a point such that the remaining runway is equal to the required safe stopping distance and has not yet reached a speed of V_1, the takeoff must be aborted. It is standard practice for pilots to reduce takeoff thrust to a level that would allow acceleration to V_1 followed by deceleration to rest such that the entire length of the runway would be used. This practice prolongs the service life of the aircraft engines and reduces the likelihood of engine failure.

Operators often use the so-called balanced field concept to calculate the lowest possible power setting for use during takeoff. Then, at speeds below V_1, there is always enough runway remaining to abort takeoff. Once V_1 is reached, the aircraft could safely takeoff even in the event of the failure of one engine. With this in mind, V_1 becomes a *decision* speed. Figure 2 shows this scenario with a takeoff rejection initiated at a decision speed of 80 m/s on a 2400 m runway.

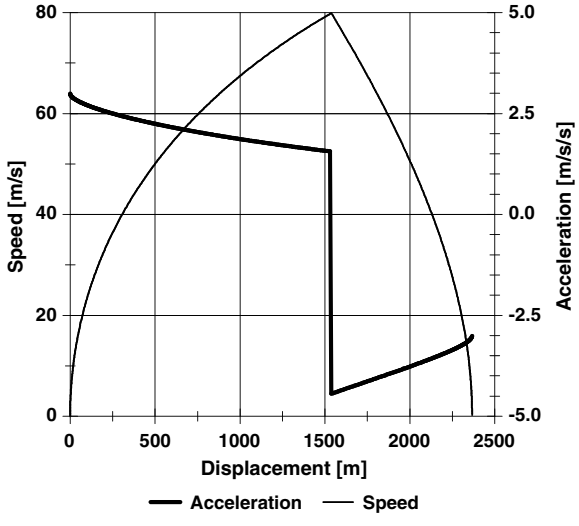

Fig. 2 Theoretical rejected takeoff.

In 1985, a study was completed at the University of Kansas [8] regarding the design of a TOPMS. By 1987 such a system was developed at NASA's Langley Research Centre for potential implementation in Boeing's B777. Simulator evaluations were completed in 1992, and flight testing [9] was performed in 1994. The proposal to include the instrument in the B777 was rejected [10] due to practical shortcomings. Specifically, there was concern over the unpredictability and variability of wind and runway conditions and the manner in which the device would compensate for this lack of information. Manufacturers predicted that the device may do more harm than good, potentially distracting the pilot unnecessarily.

A similar system for use during approach and landing is currently unavailable because of the inability for the pilot to provide remaining runway length. It is proposed that runway length information be measured independently by way of precise positioning from a GPS receiver. With this innovation, the same observer system could be used for both takeoff and landing.

II. Far-Northern Environment

The runway overrun problem is further aggravated in inclement weather where runway surfaces are contaminated by water or ice. Far-northern regions experience this sort of climate over six months of the year. Further, as such regions are relatively less populated, facilities may receive infrequent maintenance. These factors contribute to the difficulty that a pilot experiences.

Many airports in far-northern regions are gravel surfaced. The behavior of a gravel runway may be unpredictable, especially when temperatures are near the freezing point. Measurements of runway friction attempted in such conditions would be relatively unreliable.

The availability of radio navigation systems in far-northern regions is also an issue. While such facilities exist, they are sparsely distributed and tend to service the airports of major population centers. Air carriers that service airports in support of mining and forestry are less likely to have reliable access to radio navigation facilities. The use of GPS-based navigation systems has provided some relief to this problem.

Some parameters of importance in a TOPMS include wheel-bearing viscous friction, aircraft drag, runway slope, engine thrust, aircraft velocity, position relative to the end of the runway, and frictional coefficient between the aircraft tires and the runway. Previous work in the design of takeoff performance monitors [8,9] accounted for such variables individually, which led to a large uncertainty in the predicted displacement. The most significant uncertainty pertained to the measurement of runway friction coefficient. In far-northern regions, however, the majority of airports consist of gravel runways. On gravel runways, the principal means of reducing speed is through the application of reverse thrust. While braking is available to aircraft operating in these circumstances, it is used sparingly and only when absolutely necessary. As a result, a direct measurement of runway frictional coefficient may not be

needed. This serves to improve the likelihood that a monitor specifically suited to gravel runways can be successfully developed. The relative importance of the remaining parameters remains to be determined. It is expected that some parameters may be negligible and the influence of others may be combined.

III. GPS Technology

The Global Positioning System is a satellite navigation system that provides a means of calculating time, position, and velocity data using coded signals that can be processed using a receiver [11]. A minimum of four satellite signals are used to compute three-dimensional positions. A GPS receiver derives position information by measuring the time required for a signal to be transmitted from a satellite with a known position and derives velocity information by measuring the Doppler shift of the transmitted signals. There are several sources of inaccuracy in this process, including receiver noise, tropospheric delay, multipath error, satellite clock errors, orbit errors, and ionospheric delay, but the most significant effect of these combined errors relates to position errors of around 5 m without the use of differential corrections. The resulting velocity error in high-end GPS receivers used in the aerospace industry can be lower than 0.2 m/s. Furthermore, the velocity error changes slowly resulting in a virtually negligible acceleration error. With the exception of receiver noise, these errors are highly repeatable when considering time intervals of less than 1 s.

IV. Acceleration from GPS

The notion of acquiring a measurement of acceleration from a GPS receiver is not new. When compared to the measurement obtained from an accelerometer, a GPS-derived measurement of acceleration can be used to determine the gravity vector. This technique has been used in airborne gravimetry to determine the gravitational constant with accuracy [7] on the order of 10^{-5} m/s^2, but requires a substantial amount of data to filter out vibrational disturbances.

Although accelerometers have been historically used to determine aircraft acceleration, it is impossible to remove the significant and adverse influence of the gravity vector without additional instrumentation to accurately measure aircraft attitude. Accelerometers do not measure purely acceleration, but rather the force per unit mass on an element of known mass, and therefore respond to the component of gravity in the axis of sensitivity of the accelerometer. Only if the orientation of the accelerometer is well known can the influence of gravity on the accelerometer output be determined. This problem is avoided through the use of a GPS-derived measurement. This is an especially appropriate choice given the need to locate the aircraft with respect to the end of the runway, an application in which GPS technology is sensibly employed.

In aircraft landing and takeoff performance monitoring, the desired acceleration measurement should reflect the overall vehicular acceleration as opposed to vibration of subcomponents. Accelerometers are suited to measurement of vibration, where the influence of gravity need not be removed from the measurement, but a GPS-based measurement is clearly superior in stable, piecewise-constant vehicular acceleration.

It is important to note that, by virtue of the nature of the GPS signal, an accurate acceleration measurement can be obtained using a single-frequency GPS receiver. A performance monitoring system could be designed in the absence of differential corrections, which may be unavailable in far-northern regions where performance monitoring is most needed. This application of GPS technology appears to be novel.

In a recent study [1], testing was undertaken to verify the accuracy of the acceleration measurement derived from GPS data. The apparatus consisted of a vehicle-mounted GPS receiver, a bank of accelerometers, and a data acquisition system. The vehicle was rail mounted with no suspension system. Four identical accelerometers provided a confident measure of acceleration. The data acquisition system collected these data at a rate of 20 Hz, electrically synchronized with the GPS receiver's collection of raw pseudorange. During constant-speed trials, the accelerometers were used to determine the slope of the rail surface so that the influence of the gravity vector could be calculated. This slope information was cross matched with geographic location through the use of differential GPS corrections. Twenty constant-speed trials were conducted, yielding a reliable measurement of rail slope. During trials where the vehicle speed varied, the accelerometer data were corrected for the influence of minor pitch changes by subtracting the known slope at the instantaneous position. Both measurements of acceleration were filtered using the same algorithm. The GPS-derived acceleration measurement was then compared with acceleration data from the bank of accelerometers, after accounting for the effect of gravity. The standard deviation of the difference was 0.054 m/s^2. Closer analysis showed that the calculated difference was within a maximum uncertainty of 0.10 m/s^2 over 90% of the time.

V. Parametric Model

The objectives of this theoretical examination were to develop a rudimentary dynamic model of a turboprop aircraft in contact with the ground, to conduct an uncertainty analysis of the predictive aspect of the model, and to devise a signal processing technique that would permit real-time determination of model parameters. Assuming that all necessary quantities can be measured, a takeoff performance monitor would require a method to project how the speed, position, and acceleration of an aircraft might change in the future based on measurements taken in the past. This necessitates the availability of a mathematical model describing how these parameters vary with respect to one another over time. It is important to note that the model developed here is meant to be simple, yet to address the principal factors of importance. More complicated models suffer from the uncertainty in each individual factor, which together result in large overall uncertainty. In the present approach, the model is reduced to a simple set of parameters whose effect might be more accurately measured. To construct such a model, the various forces acting on the aircraft are represented as functions varying with the speed of the aircraft.

The force of drag on an aircraft,

$$D = D_3 v_{/a}^2 \tag{1}$$

where D_3 is a constant parameter for a given aircraft geometry, and $v_{/a}$ is the speed of the aircraft relative to the air.

Applying the convention that a headwind is positive and aircraft speed is positive forward,

$$D = D_3 (v_a + v)^2 \tag{2}$$

Expanding,

$$D = D_3 v_a^2 + 2D_3 v_a v + D_3 v^2 \tag{3}$$

or

$$D = D_1 + D_2 v + D_3 v^2 \tag{4}$$

where D_1, D_2, and D_3 are constant parameters for a given aircraft geometry; v_a is the component of wind in the direction of the runway; and v is the speed of the aircraft relative to the ground.

Similarly, thrust

$$T = T_0 + T_3 v_{/a}^2 \tag{5}$$

where T_0 is a parameter representing the throttle setting, and T_3 is a parameter that accounts for increased thrust at higher engine inlet air pressures.

As in the derivation for drag,

$$T = T_0 + T_3 (v_a + v)^2 \tag{6}$$

Expanding,

$$T = T_0 + T_3 v_a^2 + 2T_3 v_a v + T_3 v^2 \tag{7}$$

or

$$T = T_1 + T_2 v + T_3 v^2 \tag{8}$$

where T_1, T_2, and T_3 are constant parameters for a given throttle setting.

Simple relationships can be used for viscous friction in the landing-gear wheel bearings,

$$F = F_2 v \tag{9}$$

and for the component of weight in the direction of motion,

$$W = W_1 \tag{10}$$

where F_2 and W_1 are constants provided that the runway slope is constant. Note again that although this treatment of various relationships does not attempt to account for every possible physical effect, major influences have been considered.

Grouping similar parameters and applying Newton's second law,

$$\begin{aligned} a &= \frac{\sum F}{m} = \frac{D_1 + T_1 + W_1}{m} + \frac{D_2 + T_2 + F_2}{m} v + \frac{D_3 + T_3}{m} v^2 \\ &= P_1 + P_2 v + P_3 v^2 \end{aligned} \tag{11}$$

where m is the mass of the aircraft; P_1, P_2, and P_3 are parameters representing the net force per unit mass acting on the aircraft; and a is the acceleration of the aircraft in the direction of motion.

The result is a model relating speed and three constant parameters to acceleration. If these parameters can be directly observed based on the relationship between speed and acceleration, then the need to measure the contributing factors could be eliminated. To use this model for the prediction of later displacement requires an equation describing the displacement as a function of speed. From fundamental kinematics,

$$v = \frac{\mathrm{d}s}{\mathrm{d}t} \tag{12}$$

and

$$a = \frac{\mathrm{d}v}{\mathrm{d}t} \tag{13}$$

where s and t represent position and time, respectively. This can be solved to describe the differential time:

$$\mathrm{d}\,t = \frac{\mathrm{d}s}{v} = \frac{\mathrm{d}v}{a} \tag{14}$$

Rearranging, an equation describing the differential displacement,

$$\mathrm{d}\,s = \frac{v\,\mathrm{d}v}{a} \tag{15}$$

is found.

Incorporating the model,

$$\mathrm{d}\,s = \frac{v\,\mathrm{d}v}{P_1 + P_2 v + P_3 v^2} \tag{16}$$

If the instantaneous position and speed are known, the displacement at a reference speed can be determined through integration. The displacement

$$s_2 - s_1 = \int_{v_1}^{v_2} \frac{v\,\mathrm{d}v}{P_1 + P_2 v + P_3 v^2} \tag{17}$$

where s_1 is the instantaneous position, s_2 is the predicted position at any reference speed, v_1 is the instantaneous speed, and v_2 is the reference speed.

The solution to this integral,

$$s_2 - s_1 = \left. \frac{c\,\ell_n\,|v + c| - d\,\ell_n\,|v + d|}{P_3(c - d)} \right|_{v_1}^{v_2} \tag{18}$$

where

$$c = \frac{P_2 + \sqrt{P_2^2 - 4P_1P_3}}{2P_3} \tag{19}$$

and

$$d = \frac{P_2 - \sqrt{P_2^2 - 4P_1P_3}}{2P_3} \tag{20}$$

can be used to conduct an uncertainty analysis for the measured quantities in the model. The constants described by Eqs. (19) and (20) are used simply to make the manipulation of Eq. (18) more manageable.

VI. Uncertainty Analysis

To assess the sensitivity of the theoretical model to uncertainties in the measured quantities, an uncertainty analysis was conducted [12]. The partial derivatives of displacement with respect to the measured quantities,

$$\frac{\partial(s_2 - s_1)}{\partial v_1} = \frac{v_2 - v_1}{P_1 + P_2 v_1 + P_3 v_1^2} \tag{21}$$

$$\begin{aligned} \frac{\partial(s_2 - s_1)}{\partial P_1} &= \frac{\partial c}{\partial P_1}\left[\frac{\ell_n\,|\frac{v_2+c}{v_1+c}| + \frac{c(v_1-v_2)}{(v_1+c)(v_2+c)}}{P_3(c-d)}\right] \\ &\quad - \frac{\partial d}{\partial P_1}\left[\frac{\ell_n\,|\frac{v_2+d}{v_1+d}| + \frac{d(v_1-v_2)}{(v_1+d)(v_2+d)}}{P_3(c-d)}\right] \\ &\quad + \left(\frac{\partial d}{\partial P_1} - \frac{\partial c}{\partial P_1}\right)\left[\frac{c\,\ell_n\,|\frac{v_2+c}{v_1+c}| - d\,\ell_n\,|\frac{v_2+d}{v_1+d}|}{P_3(c-d)^2}\right] \end{aligned} \tag{22}$$

$$\begin{aligned} \frac{\partial(s_2 - s_1)}{\partial P_2} &= \frac{\partial c}{\partial P_2}\left[\frac{\ell_n\,|\frac{v_2+c}{v_1+c}| + \frac{c(v_1-v_2)}{(v_1+c)(v_2+c)}}{P_3(c-d)}\right] \\ &\quad - \frac{\partial d}{\partial P_2}\left[\frac{\ell_n\,|\frac{v_2+d}{v_1+d}| + \frac{d(v_1-v_2)}{(v_1+d)(v_2+d)}}{P_3(c-d)}\right] \\ &\quad + \left(\frac{\partial d}{\partial P_2} - \frac{\partial c}{\partial P_2}\right)\left[\frac{c\,\ell_n\,|\frac{v_2+c}{v_1+c}| - d\,\ell_n\,|\frac{v_2+d}{v_1+d}|}{P_3(c-d)^2}\right] \end{aligned} \tag{23}$$

and

$$\begin{aligned} \frac{\partial(s_2 - s_1)}{\partial P_3} &= \frac{\partial c}{\partial P_3}\left[\frac{\ell_n\,|\frac{v_2+c}{v_1+c}| + \frac{c(v_1-v_2)}{(v_1+c)(v_2+c)}}{P_3(c-d)}\right] \\ &\quad - \frac{\partial d}{\partial P_3}\left[\frac{\ell_n\,|\frac{v_2+d}{v_1+d}| + \frac{d(v_1-v_2)}{(v_1+d)(v_2+d)}}{P_3(c-d)}\right] \\ &\quad + \left(\frac{\partial d}{\partial P_3} - \frac{\partial c}{\partial P_3}\right)\left[\frac{c\,\ell_n\,|\frac{v_2+c}{v_1+c}| - d\,\ell_n\,|\frac{v_2+d}{v_1+d}|}{P_3(c-d)^2}\right] \\ &\quad + \left[\frac{c\,\ell_n\,|\frac{v_2+c}{v_1+c}| - d\,\ell_n\,|\frac{v_2+d}{v_1+d}|}{P_3^2(c-d)}\right] \end{aligned} \tag{24}$$

together with partial derivatives,

$$\frac{\partial c}{\partial P_1} = -(P_2^2 - 4P_1P_3)^{-\frac{1}{2}} \tag{25}$$

$$\frac{\partial c}{\partial P_2} = \frac{1 + P_2(P_2^2 - 4P_1P_3)^{-\frac{1}{2}}}{2P_3} \tag{26}$$

$$\frac{\partial c}{\partial P_3} = \frac{-P_2 - \sqrt{P_2^2 - 4P_1P_3} - 2P_1P_3(P_2^2 - 4P_1P_3)^{-\frac{1}{2}}}{2P_3^2} \tag{27}$$

$$\frac{\partial d}{\partial P_1} = (P_2^2 - 4P_1P_3)^{-\frac{1}{2}} \tag{28}$$

$$\frac{\partial d}{\partial P_2} = \frac{1 - P_2(P_2^2 - 4P_1P_3)^{-\frac{1}{2}}}{2P_3} \tag{29}$$

and

$$\frac{\partial d}{\partial P_3} = \frac{-P_2 + \sqrt{P_2^2 - 4P_1P_3} + 2P_1P_3(P_2^2 - 4P_1P_3)^{-\frac{1}{2}}}{2P_3^2} \tag{30}$$

form the basis of the uncertainty analysis.

An experimental investigation that was performed to validate the theoretical model is described in Pinder et al. [4]. A prototype takeoff performance monitor was installed in a 19-passenger British Aerospace 3112 operated by an airline servicing far-northern Canadian airports. The data collected in this manner were used to validate the theoretical model and to draw conclusions regarding the feasibility of implementing such a model in a takeoff performance monitor.

To establish approximate parameter values for use in the uncertainty analysis, an empirical analysis was conducted. From Eq. (11), P_3 is a function of T_3, D_3, and the mass of the aircraft. If the contribution of T_3 is neglected, it can be shown that the uncertainty in the projection of displacement is exaggerated, and therefore doing so represents a conservative approximation. The drag force on an object [13] at high Reynolds numbers,

$$D = -0.22A\rho_{\text{air}}v_{/a}^2 \tag{31}$$

where A is the frontal area of the object, ρ_{air} is the density of air, and $v_{/a}$ is the speed of the object relative to the air.

The frontal area of the BAe 3112 aircraft is 14.3 m^2. The density of air under standard sea-level conditions is 1.225 kg/m^3. The maximum allowable takeoff mass of the aircraft is 7000 kg. Neglecting T_3,

$$P_3 = \frac{D}{mv_{/\text{air}}^2} = -0.00055 \text{ m}^{-1} \tag{32}$$

Similarly, a conservative approximation of P_2 can be determined by neglecting the variability of thrust and the contribution of viscous friction in the aircraft wheel bearings. This requires an approximation of a typical yet conservatively large value for the wind speed. If this value for wind speed is chosen to be equal to 15 m/s,

$$P_2 \cong 2P_3v_a = -0.0165 \text{ s}^{-1} \tag{33}$$

Finally, choosing a nominal value for initial thrust, for the specific aircraft,

$$P_1 = 3.0 \text{ m/s}^2 \tag{34}$$

Based on these parameter values, partial derivative values are obtained:

$$\frac{\partial c}{\partial P_1} = -1.21 \times 10^1 \text{ s} \tag{35}$$

$$\frac{\partial d}{\partial P_1} = 1.21 \times 10^1 \text{ s} \tag{36}$$

$$\frac{\partial c}{\partial P_2} = -7.28 \times 10^2 \text{ m} \tag{37}$$

$$\frac{\partial d}{\partial P_2} = -1.09 \times 10^3 \text{ m} \tag{38}$$

$$\frac{\partial c}{\partial P_3} = -4.40 \times 10^4 \text{ m}^2/\text{s} \tag{39}$$

and

$$\frac{\partial d}{\partial P_3} = 9.85 \times 10^5 \text{ m}^2/\text{s} \tag{40}$$

Suppose that the aircraft in question has an instantaneous speed of 30 m/s, and the reference speed is 50 m/s. These quantities result in partial derivatives of displacement with respect to measured quantities:

$$\frac{\partial(s_2 - s_1)}{\partial v_1} = \frac{2.00 \times 10^1}{2.01} = 1.00 \times 10^1 \text{ s} \tag{41}$$

$$\frac{\partial(s_2 - s_1)}{\partial P_1} = 37.4\frac{\partial c}{\partial P_1} - 4.65\frac{\partial d}{\partial P_1} = -5.07 \times 10^2 \text{ s}^2 \tag{42}$$

$$\frac{\partial(s_2 - s_1)}{\partial P_2} = 37.4\frac{\partial c}{\partial P_2} - 4.65\frac{\partial d}{\partial P_2} = -2.22 \times 10^4 \text{ s-m} \tag{43}$$

and

$$\frac{\partial(s_2 - s_1)}{\partial P_3} = 37.4\frac{\partial c}{\partial P_3} - 4.65\frac{\partial d}{\partial P_3} - 1.12 \times 10^6 = -9.83 \times 10^5 \text{ m}^2 \tag{44}$$

These equations can be used to determine the effect of errors in the measured quantities. The specified maximum speed error for the GPS receiver was 0.20 m/s. From Eq. (41), there will exist a maximum of 2 m of error in the projected displacement due to this measurement error at the conditions outlined, and this error will decrease as the reference speed is approached.

In a conventional uncertainty analysis, each measured quantity is treated independently. In the present example, there exists only the measurement of speed provided from the GPS receiver. The remaining parameters are observed in a Kalman filter. The worst-case scenario for the observation of the parameters corresponds to a sudden change in drag coefficient or wind speed that would affect one or both of parameters P_2 and P_3 more quickly than the filter can respond. Figure 3 shows the resulting error in the projection of displacement that would occur as the aircraft accelerates from an instantaneous speed of 30 m/s to a reference speed of 50 m/s as a function of percent error in parameters P_2 and P_3. Figure 4 shows the error in projected displacement as a function of speed resulting from

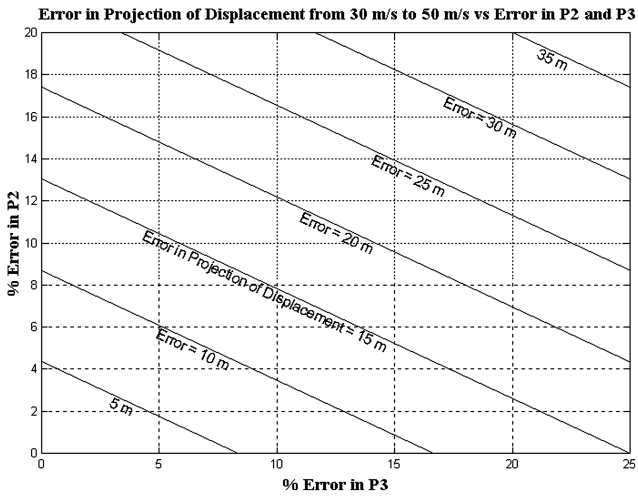

Fig. 3 Theoretical error in projection of displacement versus error in observed parameters.

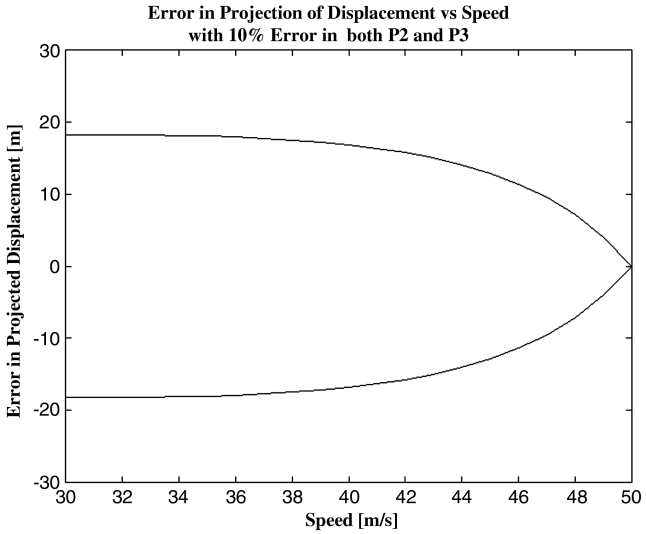

Fig. 4 Theoretical error in projection of displacement versus speed with nominal parameter error.

10% error in both parameters P_2 and P_3. As the reference speed is approached, the error in the projection of displacement that will have occurred approaches zero.

VII. Signal Processing

Customarily, the states in a Kalman filter are time derivatives of one another. This stems from the rigidity of the continuous Kalman filter, which requires that all states be related to one another through differentiation in a homogeneous domain. The discrete Kalman filter is not limited in this way. Based on the dynamics pertaining to the particular application, the designer typically chooses a high derivative to identify as a random process. The lower states are then dependent on the random variable. Each state may also be assigned some random variability to uncouple neighboring states. For instance, it would not be uncommon to describe the dynamics of an aircraft during its takeoff roll based on its position s, speed v, acceleration a, and jerk j:

$$\begin{bmatrix} s \\ v \\ a \\ j \end{bmatrix}_k = \begin{bmatrix} 1 & \Delta t & 0 & 0 \\ 0 & 1 & \Delta t & 0 \\ 0 & 0 & 1 & \Delta t \\ 0 & 0 & 0 & 0 \end{bmatrix} \begin{bmatrix} s \\ v \\ a \\ j \end{bmatrix}_{k-1} + \begin{bmatrix} 0 \\ 0 \\ 0 \\ q_j \end{bmatrix} \tag{45}$$

where Δt is the difference in time between the measurements subscripted $k-1$ and k, and q_j is a zero-mean random variable.

Such a filter functions best when jerk most closely resembles a zero-mean random process, though this is usually an approximation of reality. For small time steps, it may be considered a reasonable approximation. Note also that this requirement for small time steps results in the second and higher powers of Δt assumed negligible in the state transition matrix.

In the model,

$$a = P_1 + P_2 v + P_3 v^2 \tag{46}$$

jerk can be found through differentiation,

$$j = \frac{\mathrm{d}a}{\mathrm{d}t} = P_2 a + 2P_3 v a \tag{47}$$

or

$$j = P_1 P_2 + (P_2^2 + 2P_1 P_3)v + 3P_2 P_3 v^2 + 2P_3^2 v^3 \tag{48}$$

and is clearly not a zero-mean process, so the common approach to the implementation of a Kalman filter, described earlier, is not appropriate. The higher derivatives are also nonzero.

On the other hand, velocity derivatives of the model,

$$\frac{\mathrm{d}a}{\mathrm{d}v} = P_2 + 2P_3 v \tag{49}$$

$$\frac{\mathrm{d}^2 a}{\mathrm{d}v^2} = 2P_3 \tag{50}$$

and

$$\frac{\mathrm{d}^3 a}{\mathrm{d}v^3} = 0 \tag{51}$$

provide an alternative method of observer construction. The third velocity derivative of acceleration is a zero-mean process. Without approximation, this can be considered a random process within a Kalman filter.

Based on this knowledge, a novel observer,

$$\begin{bmatrix} s \\ v \\ a \\ \mathrm{d}a/\mathrm{d}v \\ \mathrm{d}^2a/\mathrm{d}v^2 \end{bmatrix}_k = \begin{bmatrix} 1 & \Delta t & 0 & 0 & 0 \\ 0 & 1 & \Delta t & 0 & 0 \\ 0 & 0 & 1 & \Delta v & 0 \\ 0 & 0 & 0 & 1 & \Delta v \\ 0 & 0 & 0 & 0 & 1 \end{bmatrix} \begin{bmatrix} s \\ v \\ a \\ \mathrm{d}a/\mathrm{d}v \\ \mathrm{d}^2a/\mathrm{d}v^2 \end{bmatrix}_{k-1} + \begin{bmatrix} 0 \\ 0 \\ 0 \\ q_4 \\ q_5 \end{bmatrix} \tag{52}$$

was constructed. This was a model for a Kalman filter that was capable of an optimal estimation despite reference to a nonlinear model. Note that the matrix relating state variables from one step to the next, known as the state transition matrix, contained both differential time and differential speed. As a result, the state transition matrix varied from step to step.

As a result of this signal processing technique, the predictions of the displacement of the test aircraft were accurate to within 15 m within a few seconds of the pilot finalizing control settings. This result held for 176 takeoffs recorded under varying weather conditions.

VIII. Experimental Investigation

A GPS receiver (NovAtel 3151RE) capable of collecting pseudorange measurements at a rate of 20 Hz was selected for use in the prototype takeoff performance monitor. The prototype monitor was certified for use as a global positioning data recorder (GPDR) and was installed in a 19-passenger British Aerospace 3112 operated by an airline servicing far-northern Canadian airports. The particular aircraft was equipped with a navigational GPS receiver (Bendix King KLN 89B) with a permanent active patch antenna (Bendix King KA 92) installed over the cockpit with a clear view of the sky. A signal splitter (Starlink BT-2DGPS) was installed that allowed the GPS antenna signal to be shared by the navigational GPS receiver and the GPDR. Figure 5 depicts the electrical configuration of the complete system. Figure 6 shows the internal configuration of the GPDR. The receiver contained in the GPDR logged position and velocity at a rate of 10 Hz to a portable computer that stored the data to a disk drive. The velocity measurement from the GPS receiver in the test apparatus was derived from time differentiation of position and carrier-phase Doppler measurements according to the manufacturer's proprietary algorithm.

Measurements of position and speed, obtained from a GPS receiver, were provided to the Kalman filter. The resulting states were used to calculate the parameters in the model, using Eqs. (46), (49), and (50), specifically,

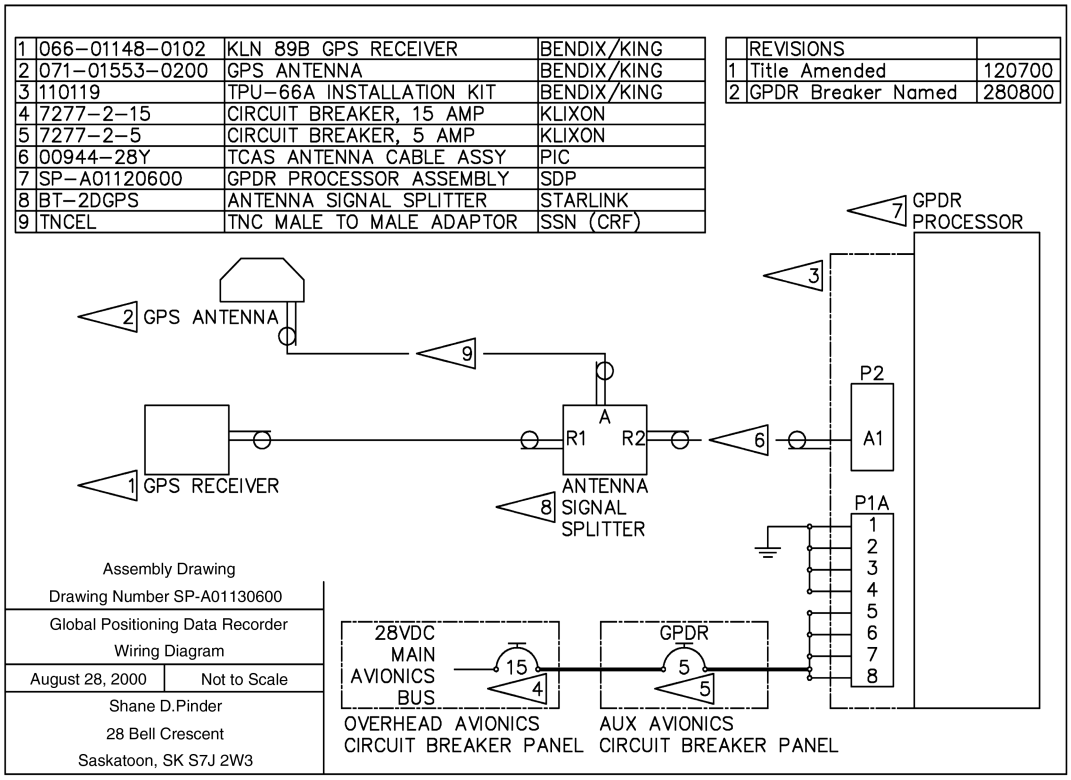

Fig. 5 System electrical schematic of global positioning data recorder.

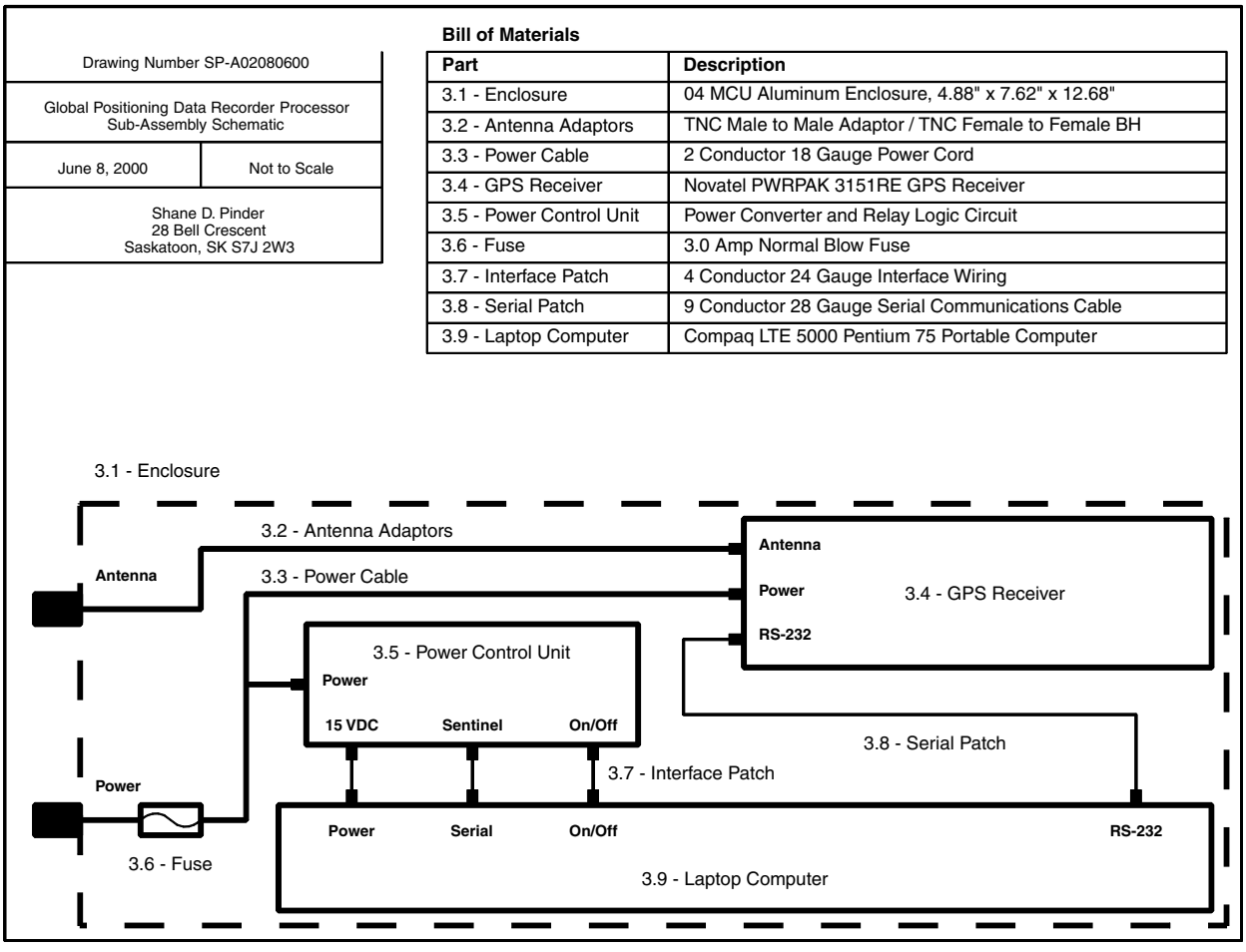

Fig. 6 Internal configuration of global positioning data recorder.

$$P_3 = \frac{1}{2}\frac{\mathrm{d}^2 a}{\mathrm{d}v^2} \tag{53}$$

$$P_2 = \frac{\mathrm{d}a}{\mathrm{d}v} - 2P_3 v \tag{54}$$

and

$$P_1 = a - P_2 v - P_3 v^2 \tag{55}$$

These observed parameter values were then used to project displacement using Eqs. (18–20).

During a typical takeoff, the aircraft begins at rest on the runway at the initial position from which future displacement is measured. After commencement of the takeoff roll, the pilot typically adjusted control settings until the aircraft had reached a speed of 25 m/s. In view of this, the signal processing technique was designed to determine parameters beginning after a speed of 30 m/s had been reached to ensure that the dynamics of the aircraft could be reasonably determined with reference to the theoretical model, which assumes that control settings do not change. Once this speed had been reached, the signal processing algorithm continuously projected the displacement that the aircraft would have at an arbitrary speed of 50 m/s. This speed was chosen as a common reference for all takeoffs, as it was always well below the rotation speed of the aircraft, and therefore the assumptions in the model would be still valid. The projected displacement was then compared with the actual displacement of the aircraft when it reached a speed of 50 m/s. The actual displacement of the aircraft was recorded from GPS data. Figure 7 shows the projected displacement determined by the estimator, and the actual instantaneous displacement, as a function of the instantaneous speed for a typical actual takeoff where the actual displacement of the aircraft reached 473 m when its speed was 50 m/s. Note that the variation during the period between 30 and 40 m/s corresponded to the time required for parameter convergence. Figure 8 shows a scatter plot of all data collected during 176 takeoffs. Note that as the speed of the aircraft approaches 50 m/s, the accuracy of the predicted displacement improves as would be expected. This diagram is intended to describe the accuracy with which displacement can be projected throughout a broad range of external factors, including varying runways, weather conditions, pilots, and times of day.

No attempt was made to limit the takeoffs included in the set of data, so the conditions experienced could best be described as typical for the particular aircraft, which made several flights daily between Saskatoon and cities with similar airports, where the runways are

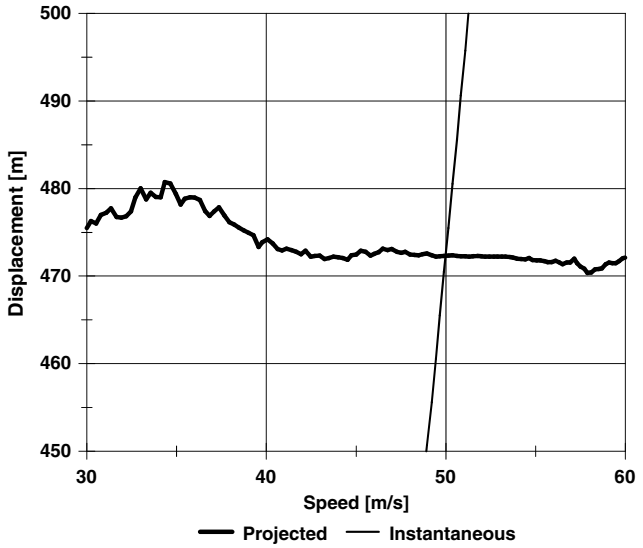

Fig. 7 During a typical takeoff, the projected displacement at a reference speed of 50 m/s converges to a value accurate to within 10 m before the aircraft has reached a speed of 35 m/s.

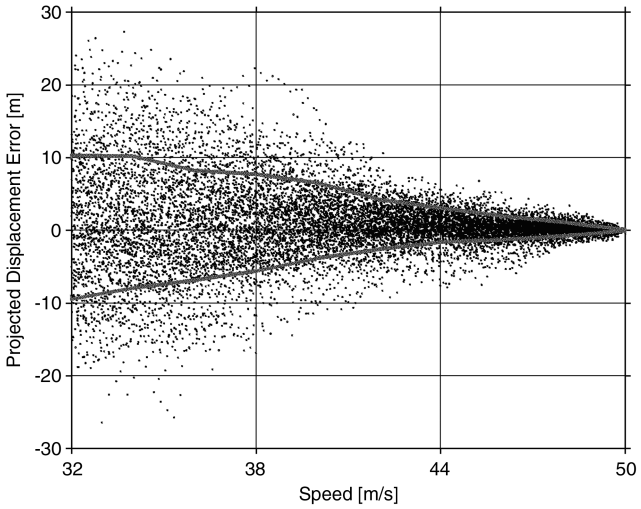

Fig. 8 Scatter plot of the error in all projection measurements determined during 176 takeoffs. The projected displacement error is the amount by which the displacement at a speed of 50 m/s differed from the instantaneous predicted displacement. The solid lines indicate the standard deviation of projected displacement error.

paved and well maintained, as well as occasional flights to remote airports with gravel runways such as Key Lake, Collins Bay, and Fond du Lac, which receive limited winter maintenance. Of the 176 takeoffs, only 16 were from gravel runways, and the sealed gravel at Stony Rapids is very similar to pavement. Runway lengths varied from 1160 to 3350 m, with gradients as much as 0.40%. Information regarding runways used is provided in Table 1. It was intended that the aircraft would visit remote airports more frequently, but this was beyond the control of the study, though future work may include such data. The data collection took place between the months of September and December, where temperatures ranged from −36 to +30°C and surface wind speeds ranged from 5 to 36 kt. Note that these were commercial flights of a 19-passenger aircraft under nominal conditions for the region served.

With regard to the parametric model, it was hypothesized that the parameter P_3 would be a characteristic of the aircraft engines and would therefore change slowly, rendering it a constant for any single takeoff. A filter with an effective time constant of several takeoffs in length was used to identify this parameter. In theory, the parameter P_2 combines the effects of runway characteristics, weather conditions, and wheel-bearing friction. A filter with a time constant a few seconds in length was used to identify this parameter. The convergence of the remaining parameter P_1 showed that this was an entirely acceptable treatment of the parameters P_3 and P_2.

IX. Limitations

The objective of this investigation was to collect data to validate a theoretical dynamic model and signal processing technique intended to be used for a TOPMS. The dynamic model was derived using simple approximations of the underlying factors and resulted in the identification of three parameters that represent the combined effect of many otherwise measurable factors. We hypothesized that determining the value of each of these parameters through instantaneous observation of the combined effect could yield a better projection of displacement than might be possible from accounting for a litany of underlying factors whose combined uncertainty could be large.

We collected data during typical takeoffs of one aircraft, a BAe 3112. While the results appear promising for this aircraft, we do not speculate as to how well this model will perform with other aircraft or other classes of aircraft.

In the measure of the performance of the model and the approach to observation, only the error in projected displacement during the phase of the takeoff where the aircraft accelerates to the rotation speed has been considered, though this is appropriate given that the

Table 1 Runway information, including the number of takeoffs recorded

Name	Latitude	Longitude	Length, m (ft)	Width, m (ft)	Runway (takeoffs)		Surface
Fond du Lac	N59 20 01	W107 10 56	1160 (3800)	23 (75)	10 (4)	28 (0)	Gravel
Stony Rapids	N59 15 01	W105 50 29	1540 (5050)	30 (100)	06 (2)	24 (5)	Sealed gravel
Collins Bay	N58 14 10	W103 40 39	1580 (5200)	34 (110)	02 (1)	20 (2)	Gravel
Key Lake	N57 15 23	W105 37 03	1610 (5280)	60 (200)	03 (2)	21 (0)	Gravel
La Ronge	N55 09 05	W105 15 43	1525 (5000)	45 (150)	18 (8)	36 (7)	Asphalt
Edmonton	N53 34 21	W113 31 14	1740 (5700)	60 (200)	16 (2)	34 (2)	Asphalt
Edmonton	N53 34 21	W113 31 14	1790 (5868)	60 (200)	12 (0)	30 (1)	Asphalt
Prince Albert	N53 12 51	W105 40 22	1525 (5000)	60 (200)	08 (9)	26 (8)	Asphalt
Saskatoon	N52 10 15	W106 41 59	1890 (6200)	45 (150)	15 (17)	33 (9)	Asphalt
Saskatoon	N52 10 15	W106 41 59	2530 (8300)	60 (200)	09 (18)	27 (11)	Asphalt
Regina	N50 25 55	W104 39 57	1890 (6200)	45 (150)	08 (1)	26 (3)	Asphalt
Regina	N50 25 55	W104 39 57	2410 (7900)	45 (150)	13 (19)	31 (20)	Asphalt
Brandon	N49 54 36	W099 57 07	1980 (6500)	45 (150)	08 (6)	26 (6)	Asphalt
Winnipeg	N49 54 39	W097 14 36	1400 (4600)	60 (200)	07 (0)	25 (9)	Asphalt
Winnipeg	N49 54 39	W097 14 36	2650 (8700)	60 (200)	13 (0)	31 (1)	Asphalt
Winnipeg	N49 54 39	W097 14 36	3350 (11000)	60 (200)	18 (1)	36 (1)	Asphalt

displacement during the deceleration phase ought to be conservatively chosen given the possible causes of the rejection of a takeoff. Further, we have not described how advisory information might be generated from the model.

While it is considered in ongoing research, the greatest limitation in this work is the need to consider the human response required. It should seem as though the model put forward, in actuality, is far more accurate than necessary, given that the uncertainty in projected displacement would be consumed in a fraction of a second of pilot reaction time. Therefore, the manner in which the information is conveyed to the pilot is far more important than any further improvement in model accuracy.

X. Future Work

Ongoing research in this field includes the development of a bimodal cockpit human–machine interface [14] and the validation of a device intended to be used as an advisor for both takeoff and landing. In this ongoing development of the technology, the instrument is designed to take advantage of existing knowledge and procedures and to both reinforce existing procedures and to train the flight crew for rare events.

Visual presentation of information is actively used in the cockpit. The pilot must continuously monitor both cockpit instruments and the external forward environment while at the same time physically controlling the aircraft and maintaining awareness of cockpit communication. An ability to evaluate the visual environment while being provided the information from the display in an auditory manner may ease the cognitive burden of the pilot.

In many circumstances the method of alerting the pilot to a low power situation is for the copilot to verbally communicate, "low power." As auditory information can only be maintained in the memory for a short time, it often takes precedence over visual displays. As sound is preattentive, requiring less concentration and resulting in an instinctive response, auditory displays may be advantageous [15].

In emergency situations pilots must readily respond to information. Most systems currently use verbal communication to indicate danger. For instance, a ground-proximity warning system alerts the pilot of the possibility of ground collision with the verbal warning, "terrain." The effect of voice characteristics [16] on performance of the pilot, such as response time and the suitability of the response, are particularly important considerations in a time-and-space-limited scenario such as takeoff or landing. In the deployment of new systems, the use of verbal commands has the added benefit of training the pilot while in flight.

A dual display, incorporating both audible and visual information, is advantageous as the mental workload is distributed across the two modalities. The channels required to process visual information are different than those to process auditory information. By providing different information to each of the senses, the workload may be reduced. This allows for information to be displayed quickly, but a matching visual message with more precise information can be attended to after higher priority tasks have been completed.

The role of the device under development, the thrust and braking indicator/advisor (TABI/A) is twofold: provide status information regarding the progress of the landing or takeoff, and issue alerts to allow the pilot to control the aircraft such that dangerous situations are avoided. The selected interface provides status information visually, which could be scanned by the flight crew in the same way as other cockpit instruments are viewed. Verbal warnings are issued a few seconds before the pilot must make an appropriate control adjustment. In the event that the pilot has not selected a thrust or braking setting resulting in a safe acceleration, the TABI/A will issue an audible alert. In the case of takeoff, a verbal alert of "low power" is issued a few seconds before maximum thrust must be selected to safely complete the takeoff.

XI. Conclusions

The aircraft in this experimental investigation measured 15 m from nose to tail. From the data collected, it was concluded that a projection of displacement can be determined to within an uncertainty of 15 m in sufficient time to alert the pilot of an unsafe situation. While it is widely understood that many factors influence the motion of an aircraft in contact with the ground, the proposed model suggests that the sufficient information exists in GPS-derived data to instantaneously and continuously determine three parameters that can be used to adequately predict the distance required to reach any particular speed. These three parameters take into account the majority of factors affecting the motion of the aircraft.

The use of a parametric model in conjunction with a carefully designed Kalman filter has made it possible to design a prototype takeoff performance monitor that is less susceptible to the uncertainties present in the factors affecting an aircraft during takeoff. While it remains to be determined whether this level of accuracy will be attainable on other similar aircraft, it appears likely that a takeoff performance monitor designed for turboprop aircraft on gravel runways will be capable of predicting displacement with a level of uncertainty approximately equal to the length of the aircraft, which is a particularly stringent benchmark. The uncertainty analysis that was conducted has been shown to be valid for a particular aircraft operating on varied runways.

In early TOPMS work, concerns were raised over uncertainty in the predictive aspects of algorithms and the likelihood that this would lead to nuisance alerts. This stigma appears to continue in the aerospace community over 20 years later, but this concern is misplaced. It is not the accuracy with which any particular technique can predict the future that is problematic, as this is by far the smallest contributor to uncertainty. The reaction time of the pilot and the manner in which advisory information is provided should be of far

greater concern. The aerospace community has made great advances in these fields in the past 20 years.

Acknowledgments

The management and maintenance staff of Transwest Air generously provided crucial advice as well as space onboard a Jetstream 31 aircraft for the installation of the global positioning data recorder. Neil Larsen and Jonathan Tonn deserve special thanks. Daniel Aspel of TRLabs, Saskatoon, provided collaborative technical support. Their efforts are sincerely appreciated.

References

[1] Pinder, S. D., Crowe, T. G., and Nikiforuk, P. N., "Application of the Global Positioning System in Determination of Vehicular Acceleration," *Journal of Aircraft*, Vol. 38, No. 5, 2001, pp. 856–859. doi:10.2514/2.2844

[2] "TSB Statistical Summary, Aviation Occurrences, 1996," Transportation Safety Board of Canada, 1997.

[3] "Reduced Power at Takeoff and Collision with Terrain," Transportation Safety Board of Canada, Rept. A04H0004, 2006.

[4] Pinder, S. D., Crowe, T. G., and Nikiforuk, P. N., "A Practical Investigation of a Takeoff Performance Monitor for Turboprop Aircraft," *AIAA Guidance, Navigation, and Control Conference* [CD-ROM], AIAA, Reston, VA, Aug. 2001.

[5] Zammit-Mangion, D., and Eshelby, M., "Evaluation of Takeoff Performance Monitoring Algorithm in Large Jet Transport Operations," *Journal of Aircraft*, Vol. 43, No. 1, 2006, pp. 201–206. doi:10.2514/1.2974

[6] Zammit-Mangion, D., and Eshelby, M., "Improved Algorithm for Takeoff Monitoring," *Journal of Aircraft*, Vol. 44, No. 2, 2007, pp. 386–392. doi:10.2514/1.14989

[7] Wagenmakers, J., *Aircraft Performance Engineering*, Prentice–Hall, New York, 1991.

[8] Srivatsan, R., "Design of a Takeoff Performance Monitoring System," Ph.D. Dissertation, Univ. of Kansas, Lawrence, KS, 1985.

[9] Middleton, D. B., Srivatsan, R., and Person, L. H., Jr., "Flight Test of Takeoff Performance Monitoring System," NASA TP-3403, 1994.

[10] Wallace, L. E., "Airborne Trailblazer—Two Decades with NASA Langley's 737 Flying Laboratory," NASA SP-4216, 1993.

[11] Spilker, J. J., Jr., "Overview of GPS Operation and Design," *Global Positioning System: Theory and Applications*, edited by B. W. Parkinson, and J. J. Spilker Jr., Vol. 1, AIAA, Washington, D.C., 1996, pp. 29–56.

[12] Pinder, S. D., "Aircraft Takeoff Performance Monitoring in Far-Northern Regions," Ph.D. Dissertation, Univ. of Saskatchewan, Saskatchewan, Canada, 2001.

[13] Gaskell, D. R., *An Introduction to Transport Phenomena in Engineering*, Macmillan, New York, 1992, p. 160.

[14] Pinder, S. D., Bristow, D. N., and Davies, T. C., "Interface Design for and Aircraft Thrust and Braking Indicator/Advisor," *HFESA Computer-Human Interaction Conference*, Nov. 2006.

[15] Wickens, C. D., Goh, J., Helleberg, J., Horrey, W. J., and Talleur, D. A., "Attentional Models of Multitask Pilot Performance Using Advanced Display Technology," *Human Factors*, Vol. 45, 2003, pp. 360–380. doi:10.1518/hfes.45.3.360.27250

[16] Arrabito, G. R., "Effects of Talker Sex and Voice Style of Verbal Cockpit Warnings on Performance," *Human Factors*, Vol. 51, 2009, pp. 3–20. doi:10.1177/0018720808333411